Electronic Supplementary Information

A pyridine based Schiff base as a selective and sensitive fluorescent probe for cadmium ions with "turn-on" fluorescence responses

Jialin Ma,[a] Yuwei Dong,*[a] Zhou Yu,[a] Yan Wu,[b] and Zhen Zhao,*[a,c]

[a] Institute of Catalysis for Energy and Environment, College of Chemistry & Chemical Engineering, Shenyang Normal University, Shenyang, Liaoning 110034, P. R. China

[b] Qiqihar Medical University, Qiqihar, Heilongjiang 161006, P. R. China

[c] State Key Laboratory of Heavy Oil Processing, College of Science, China University of Petroleum, Beijing 102249, P. R. China

E-mail: ywdong@synu.edu.cn and zhenzhao@cup.edu.cn

Index

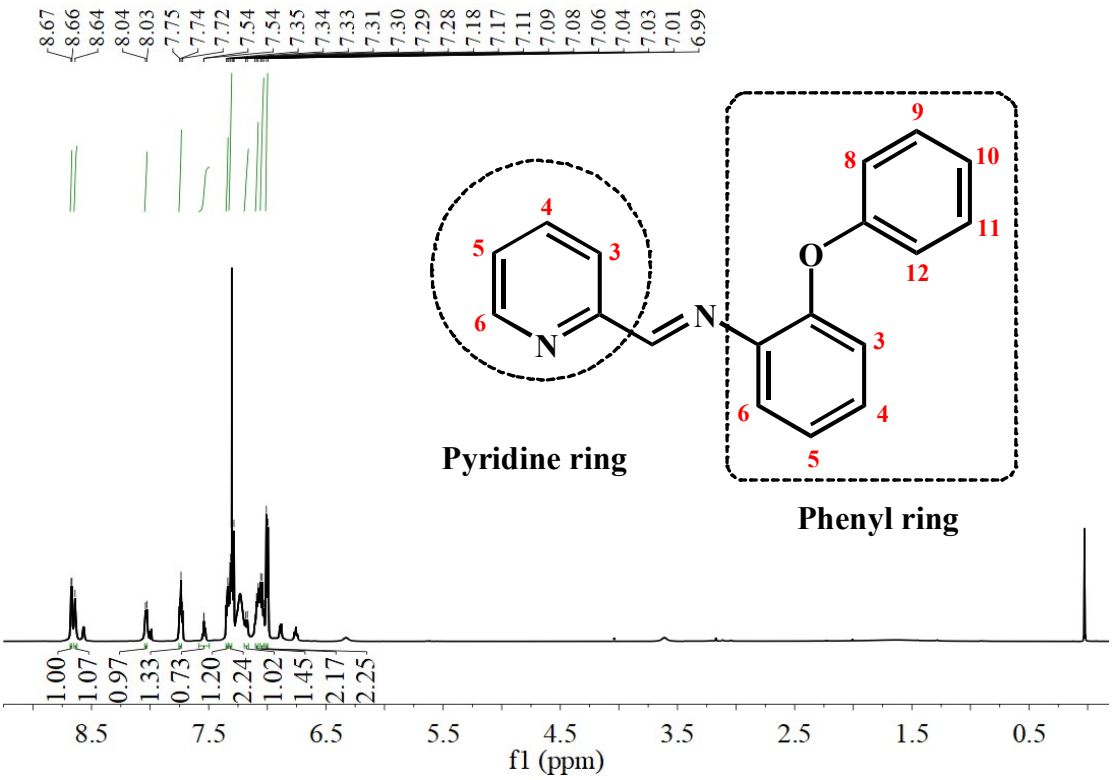

Figure S1. ^{1}H NMR spectrum of probe **PMPA** in $CDCl_3$.

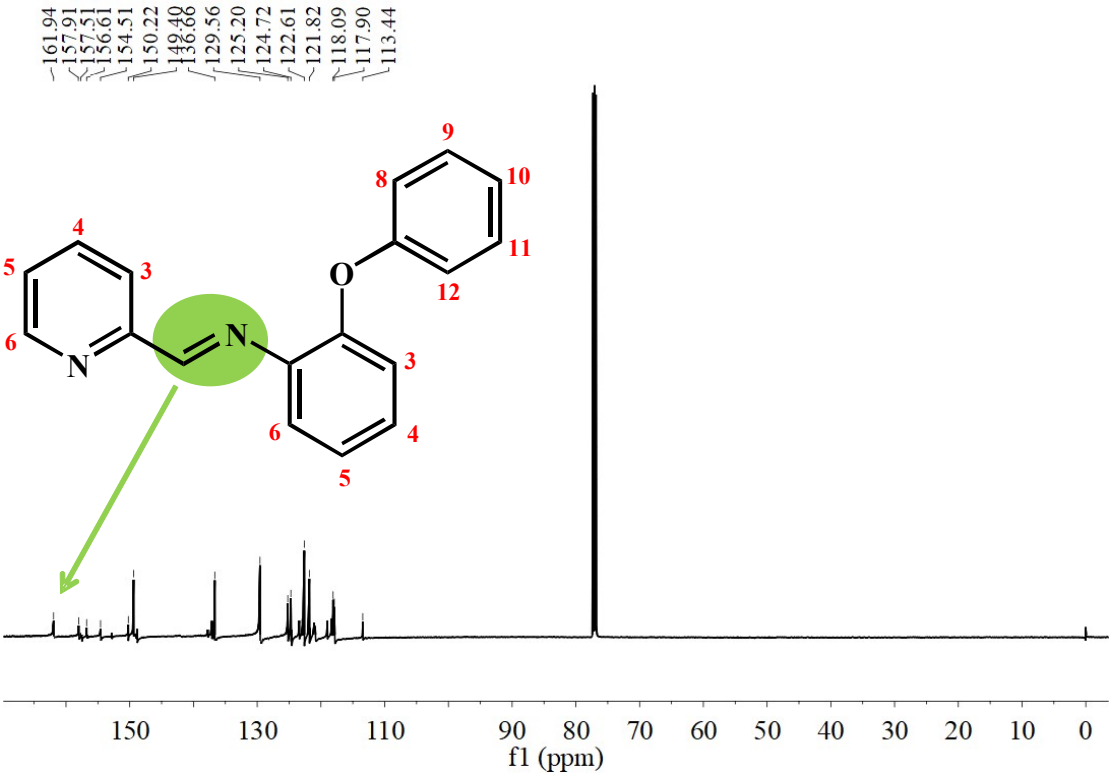

Figure S2. ^{13}C NMR spectrum of probe **PMPA** in $CDCl_3$.

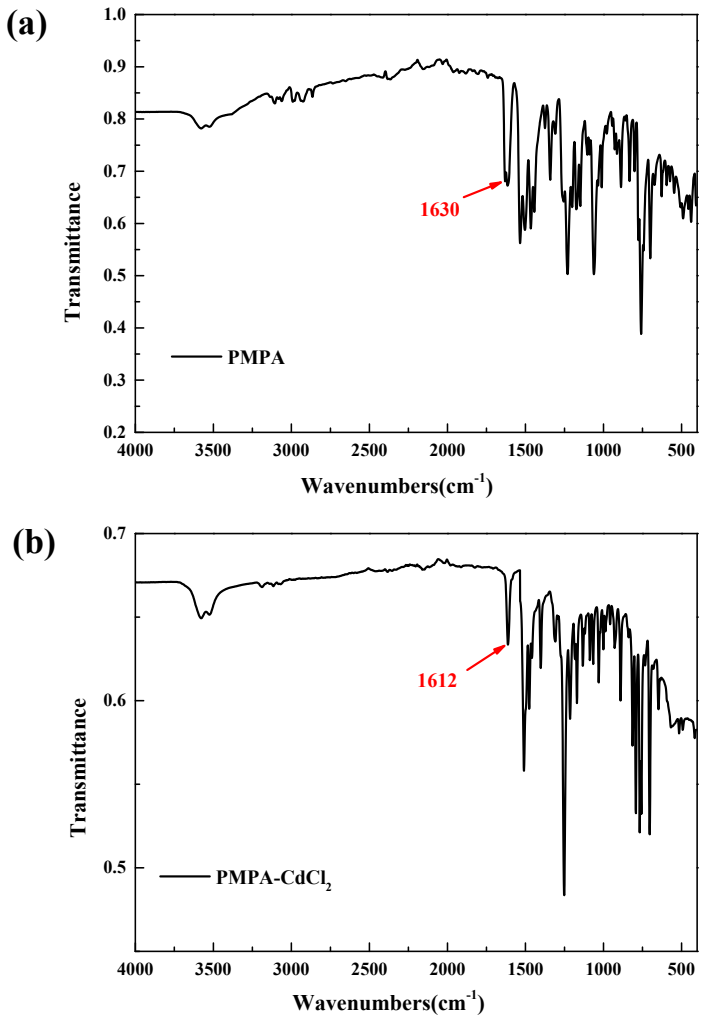

Figure S3. FT–IR spectra of (a) probe **PMPA** and (b) complex **PMPA−$CdCl_2$**.

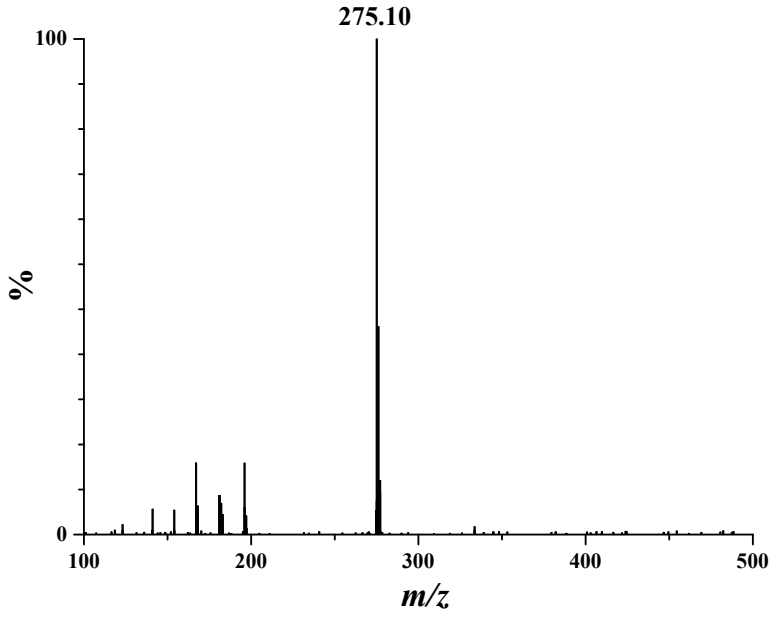

Figure S4. ESI–MS spectrum of probe **PMPA**.

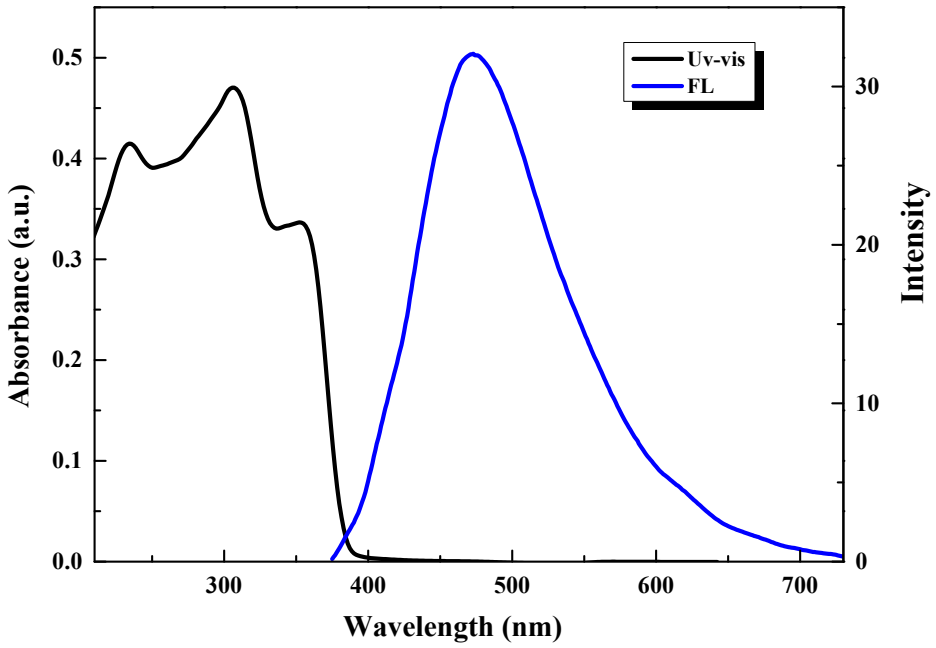

Figure S5. Absorption spectra (black line) and fluorescence emission spectra (blue line) of probe **PMPA** in acetonitrile solvent. The concentration was maintained at 10 μM.

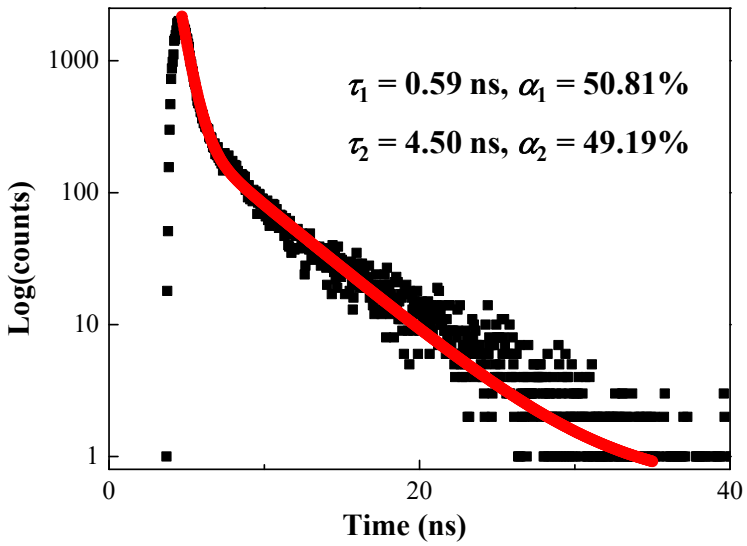

Figure S6. Fluorescence decay profile for probe **PMPA** in acetonitrile solution (λ_{ex} = 380 nm, λ_{em} = 468 nm).

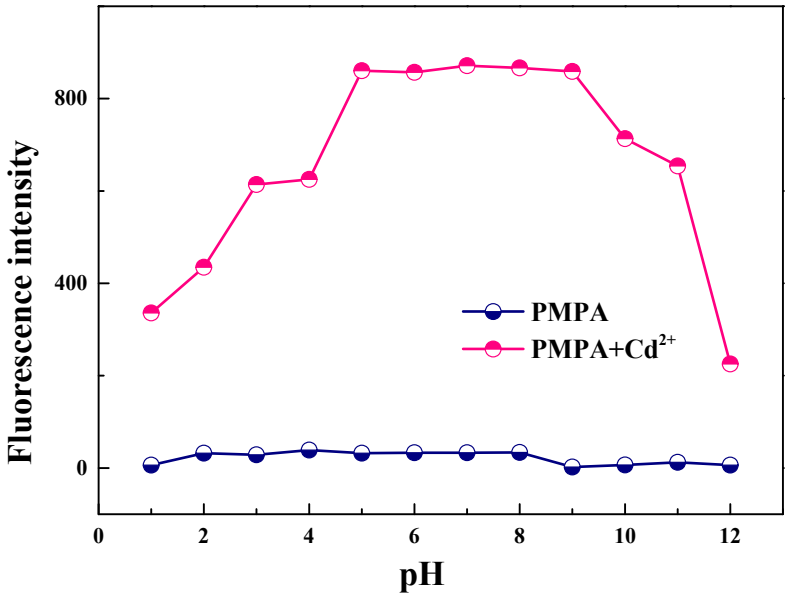

Figure S7. The fluorescence intensity of **PMPA** and **PMPA**+Cd^{2+} at different pH (1–12).

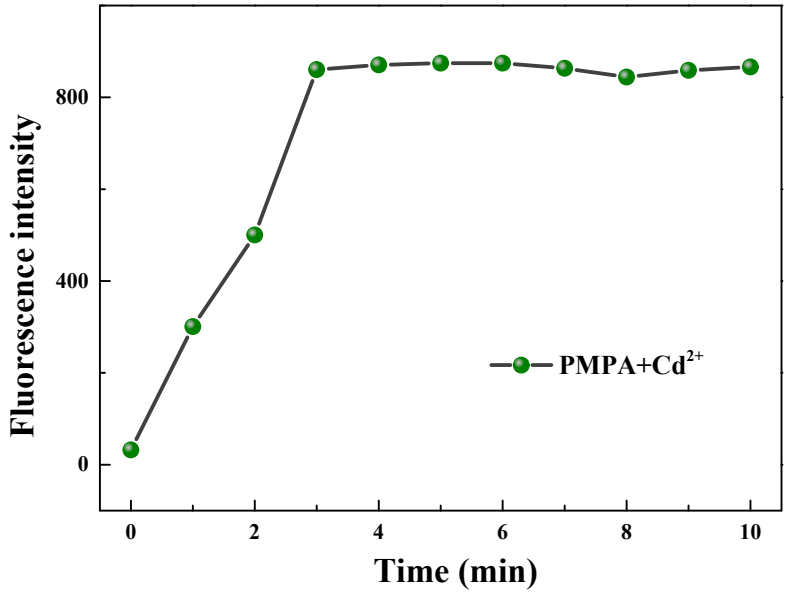

Figure S8. The effect of response time on the fluorescence intensity of **PMPA** over the addition of Cd^{2+} (at 506 nm).

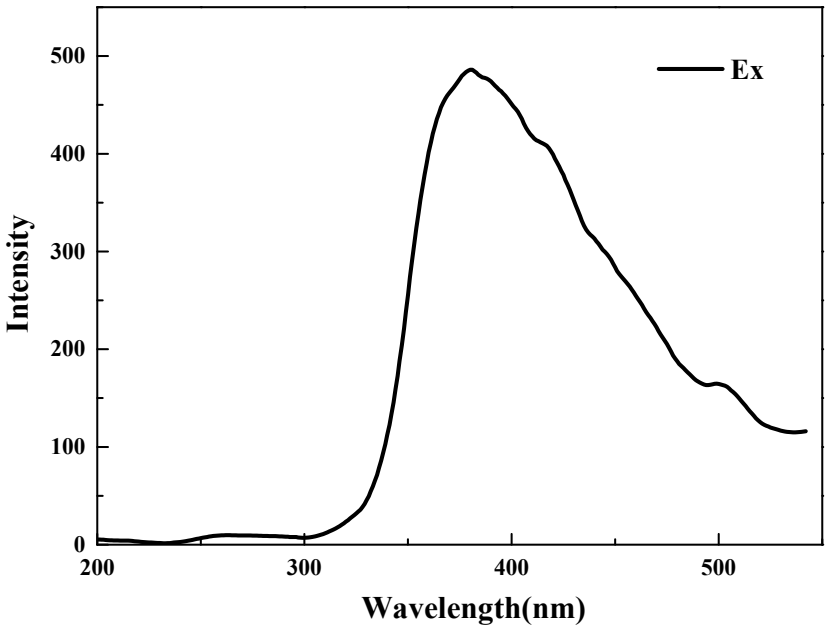

Figure S9. The excitation spectrum of probe **PMPA** upon addition of Cd^{2+}.

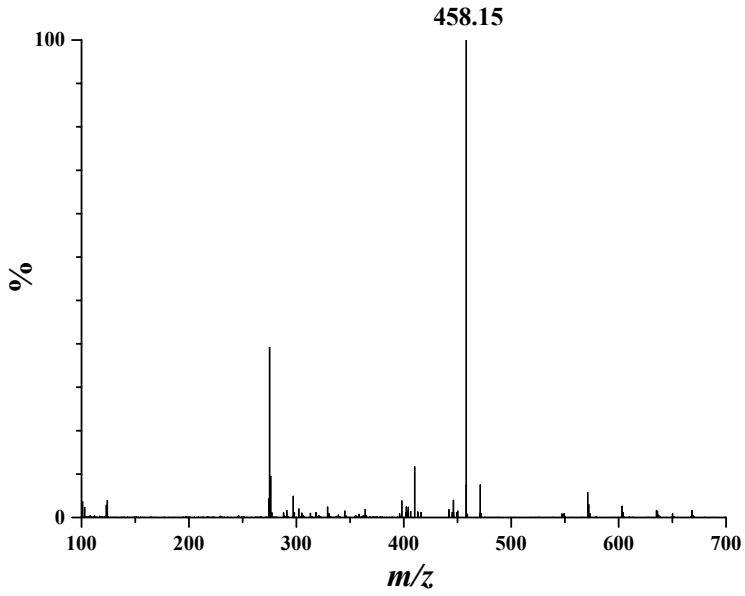

Figure S10. ESI–MS spectrum of the complex **PMPA−$CdCl_2$**.

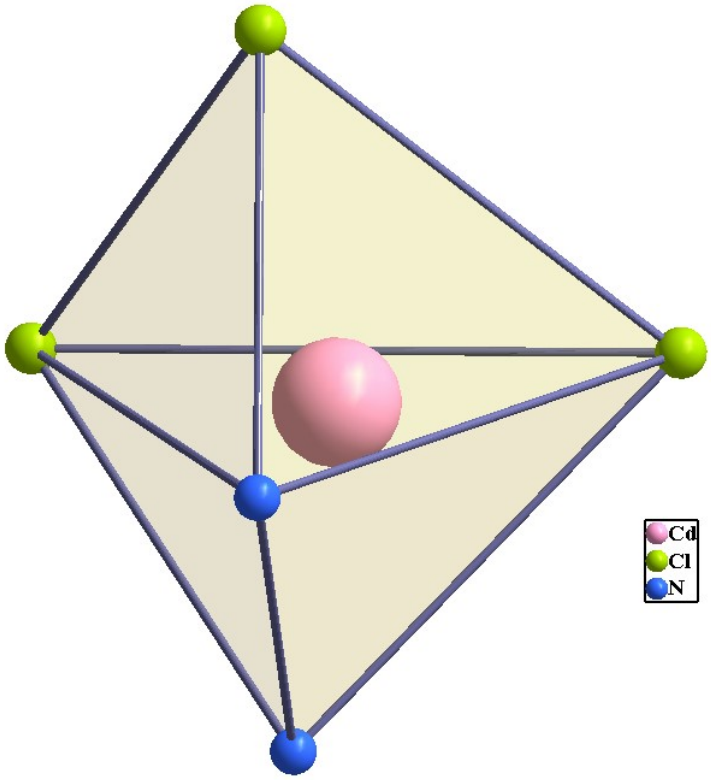

Figure S11. Coordination geometry of cadmium(II) ions in the complex **PMPA−$CdCl_2$**.

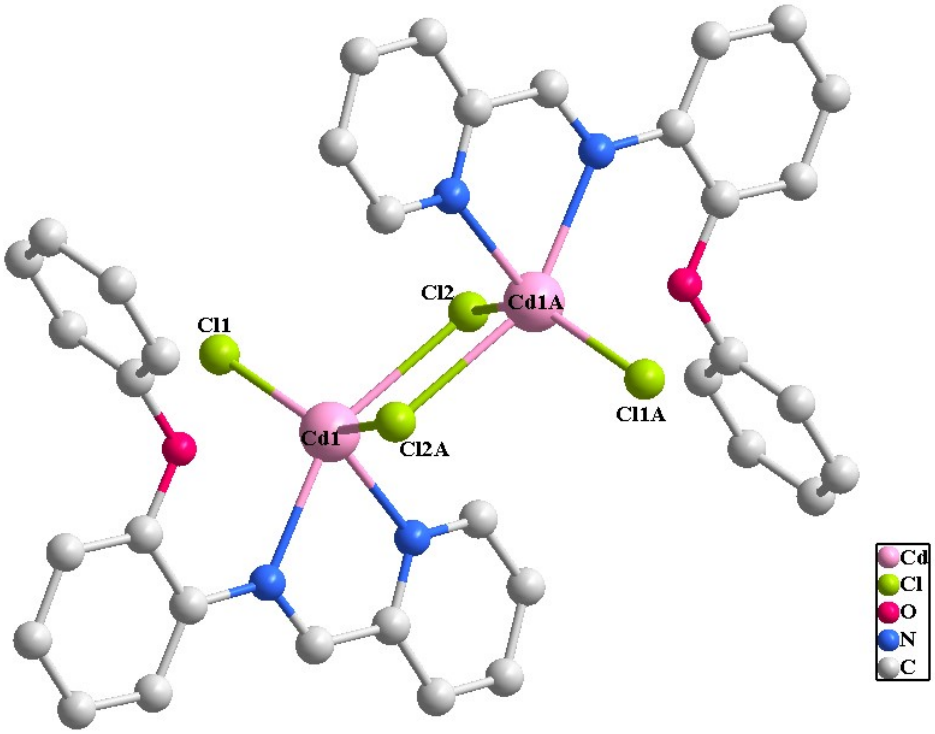

Figure S12. The binuclear unit of the complex **PMPA−$CdCl_2$**.

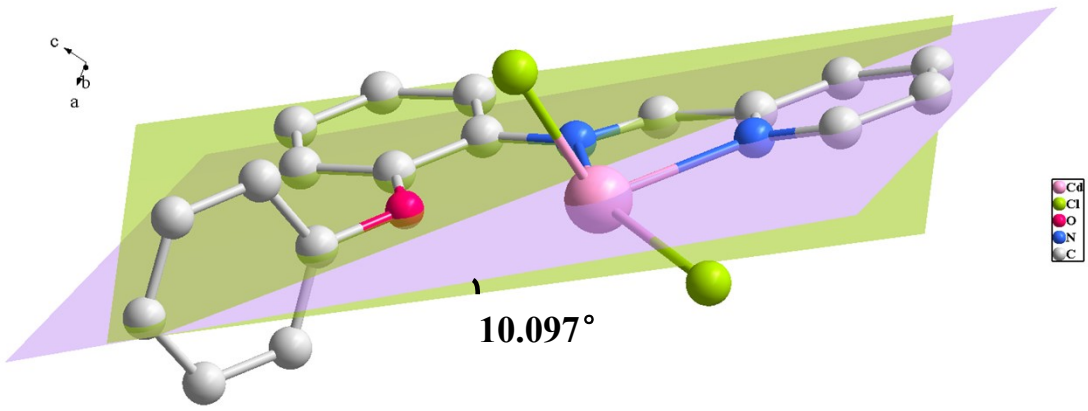

Figure S13. Depiction of the dihedral angle between the pyridine ring and the phenyl ring in the complex **PMPA−$CdCl_2$**.

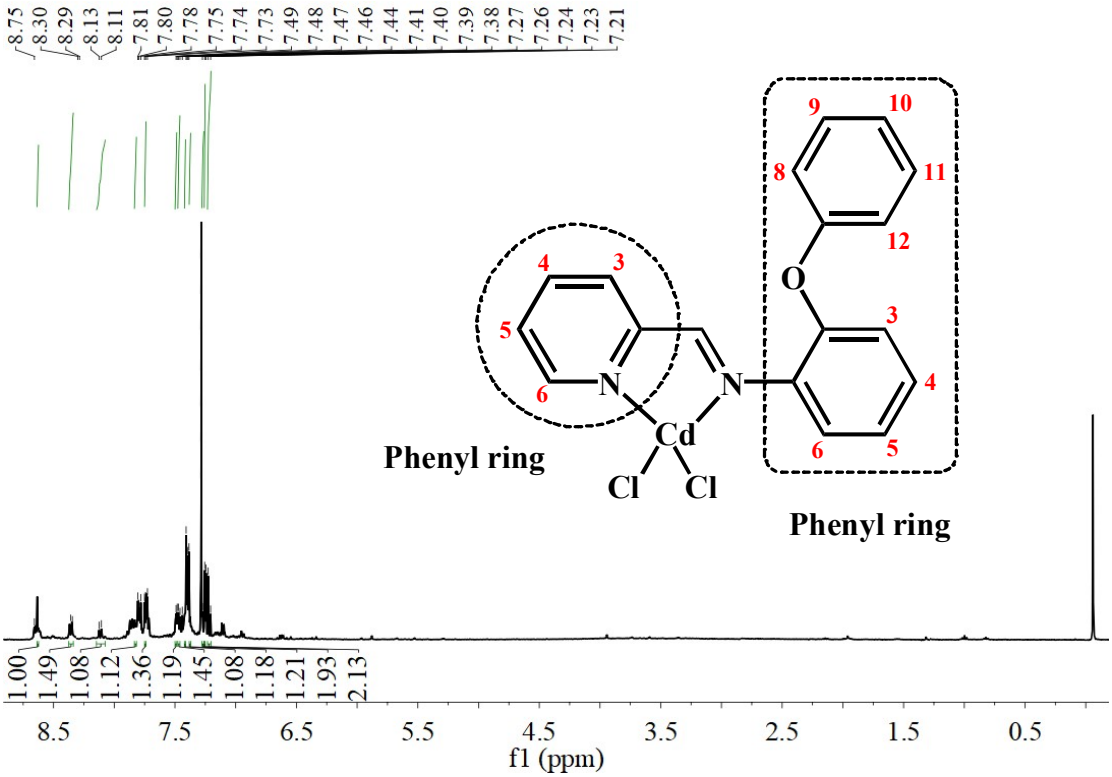

Figure S14. ^{1}H NMR spectrum of the complex **PMPA−$CdCl_2$** in $CDCl_3$.

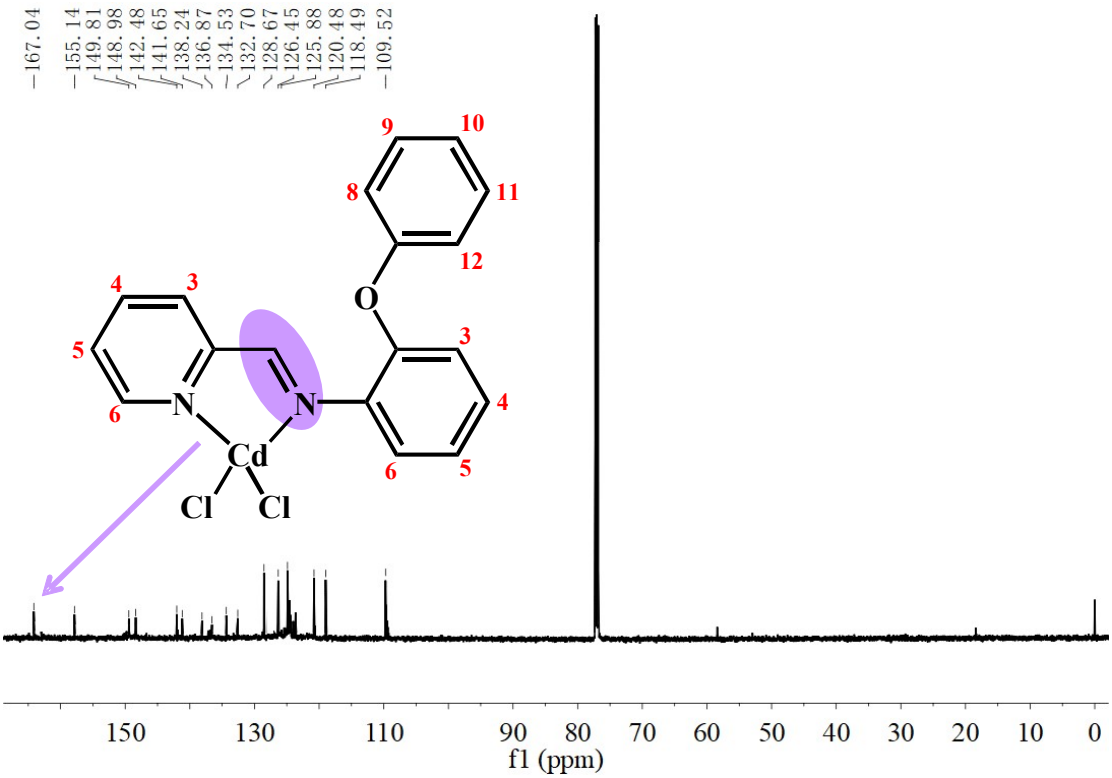

Figure S15. ^{13}C NMR spectrum of the complex **PMPA−$CdCl_2$** in $CDCl_3$.

Standard deviation and detection limit calculation

The detection limit was calculated based on the fluorescence titration. To determine the S/N ratio, fluorescence intensity of **PMPA** without Cd^{2+} was measured by five times and the standard deviation of blank measurements was determined. To gain the slop, the fluorescence intensity data at 479 nm for Cd^{2+}, were plotted as a concentration of Cd^{2+}. So the detection limit was calculated with the follow equation (1):

$$\text{Detection limit} = 3\sigma/m \quad (1)$$

Where σ is the standard deviation of blank measurements, and m is the slop of fluorescence versus Cd^{2+} concentration.

Table S1. Standard deviation calculation.

	Fluorescence intensity
Test 1	32.24
Test 2	28.67
Test 3	38.95
Test 4	32.27
Test 5	33.03
Standard Deviation (σ)	3.72

Table S2. Crystallographic and structural determination data for the complex **PMPA–$CdCl_2$**.

	PMPA–$CdCl_2$
CCDC No.	2122596
formula	$C_{18}H_{14}Cl_2N_2OCd$
Mr	457.61
A cryst syst	Triclinic
space group	*P*–1
a [Å]	8.0895(2)
b [Å]	8.7415(2)
c [Å]	13.3578(3)
α [°]	108.358(2)
β [°]	96.423(2)
γ [°]	97.449(2)
Volume [Å^3]	877.17(4)
Z	2
D_c [g·cm^{-3}]	1.733
μ [mm^{-1}]	12.827
F (000)	452
Θ range [°]	3.533 – 68.293
h range	$-9 \le h \le 6$
k range	$-10 \le k \le 10$
l range	$-15 \le l \le 15$
data/restraints/params	3102 / 0 / 217
GOF	1.040
R_1, wR_2[I>2σ(I)][a]	0.0474, 0.1220
R_1, wR_2[all data][a]	0.0487, 0.1234
$\Delta\rho_{max}$, $\Delta\rho_{min}$ [e·Å^{-3}]	0.977, –1.985

[a] $R_1 = \sum||F_o| - |F_c||/\sum|F_o|$; $wR_2 = [\sum[w\,(F_o^2 - F_c^2)^2]/\sum[\,w\,(F_o^2)^2]]^{1/2}$.

Table S3. Selected bond distances (Å) and angles (°) for the complex **PMPA–$CdCl_2$**.

Parameter	**PMPA–$CdCl_2$**
Cd(1)-N(1)	2.338(4)
Cd(1)-N(2)	2.423(3)
Cd(1)-Cl(1)	2.4090(13)
Cd(1)-Cl(2)	2.7424(10)
Cd(1)-Cl(2A)	2.5140(11)
N(2)-C(6)	1.265(6)
N(2)-Cd(1)-N(1)	70.93(12)
N(1)-Cd(1)-Cl(1)	110.93(10)
N(2)-Cd(1)-Cl(1)	105.29(9)
N(1)-Cd(1)-Cl(2)	86.40(9)
N(2)-Cd(1)-Cl(2)	153.76(9)
Cl(2)-Cd(1)-Cl(1)	94.87(4)
N(1)-Cd(1)-Cl(2A)	109.59(10)
N(2)-Cd(1)-Cl(2A)	93.19(9)
Cl(2)-Cd(1)-Cl(2A)	81.86(3)
Cl(2A)-Cd(1)-Cl(1)	139.04(4)
C(1)-N(1)-Cd(1)	115.7(3)
C(5)-N(1)-Cd(1)	126.2(3)
C(6)-N(2)-Cd(1)	112.8(3)
C(12)-N(2)-Cd(1)	127.1(3)

Table S4. Determinations of Cd^{2+} in real samples (n = 3).

Sample	Added (μM)	Measure (μM)	Recovery (%)	RSD (%)
Tap water	0	0	—	—
	3	2.56	85.33	0.945
Pond water	0	0	—	—
	3	1.85	61.67	1.470
Hun River water	0	0	—	—
	3	1.57	52.67	1.236